Engineering Conferences International
ECI Digital Archives

The 14th International Conference on Fluidization – From Fundamentals to Products

Refereed Proceedings

2013

# Modelling the Transition to the Fluidized State of Two-Solid Beds: Mixtures of Particles of Irregular Shape

Brunello Formisani
*University of Calabria, Italy*

Rossella Girimonte
*University of Calabria, Italy*

Vincenzino Vivacqua
*University of Calabria, Italy*

# MODELLING THE TRANSITION TO THE FLUIDIZED STATE OF TWO-SOLID BEDS: MIXTURES OF PARTICLES OF IRREGULAR SHAPE

Brunello Formisani[a]*, Rossella Girimonte[a] and Vincenzino Vivacqua[a]
[a]University of Calabria; Dept. Chemical Engineering and Materials
87030 Arcavacata di Rende (Cosenza), Italy
*T: +39-0984-496691; F: +39-0984-496655; E: bruno.formisani@unical.it

**ABSTRACT**
The analysis of experiments conducted on binary beds of irregular-shaped solids, such as biomass granules (crushed olive pits) and sand, shows that a recent model devised for predicting the initial and final fluidization velocity of a two-component bed of spherical solids captures also the behaviour of mixtures of non-spherical particles.

**INTRODUCTION**
In a previous work (1), fluidization of two-solid beds has been subjected to fundamental analysis. This approach has led to the development of a model capable of interpreting the behaviour of binary-solid systems where segregation is driven by either size or density difference of their components. Based on a fundamental force balance, this model provides relationships for the velocity thresholds which encompass the fluidization process, namely the ''initial'' and the ''final fluidization velocity'' of the mixture, hereafter referred to as $u_{if}$ and $u_{ff}$, respectively. $u_{if}$ is predicted by means of a fully theoretical equation, whereas just one parameter is needed to calculate $u_{ff}$. Although not thoroughly predictive as for the evaluation of $u_{ff}$, the model equations have proved to be accurate in reproducing the dependence of either characteristic velocity on solid properties and mixture composition. A remarkable feature of the approach proposed is that of offering a unique interpretation frame of two-solid fluidization, overcoming the need for the separated analysis which characterizes previous literature works (3-6).

More recently, the validity of the approach proposed has been successfully checked on beds of fully dissimilar solids (2), where both density and size differences are at work in promoting component separation. In this case, the simultaneous action of these two effects can give place to different segregation patterns. Like with particles that differ either in density or size, whenever these factors act synergistically (i.e when the larger particles are also denser), the progress of fluidization in an initially well-mixed system is accompanied by segregation mechanisms which determine the bed structure sketched in Fig.1a and described in detail elsewhere (1,2). This phenomenology has been termed "top fluidization", since by increasing the gas velocity over $u_{if}$ the fluidized portion of the bed widens downward from the bed surface, while a static bed forms at the base. Conversely, with binary systems whose denser component is also the smaller, more than one fluidization patterns is possible. If the denser solid

achieves fluidization first, the fluidization front may develop at the bottom of the bed (Fig. 1b) and the whole phenomenology is somewhat reversed, so that it can be referred to as ‘‘bottom fluidization’ (2).’

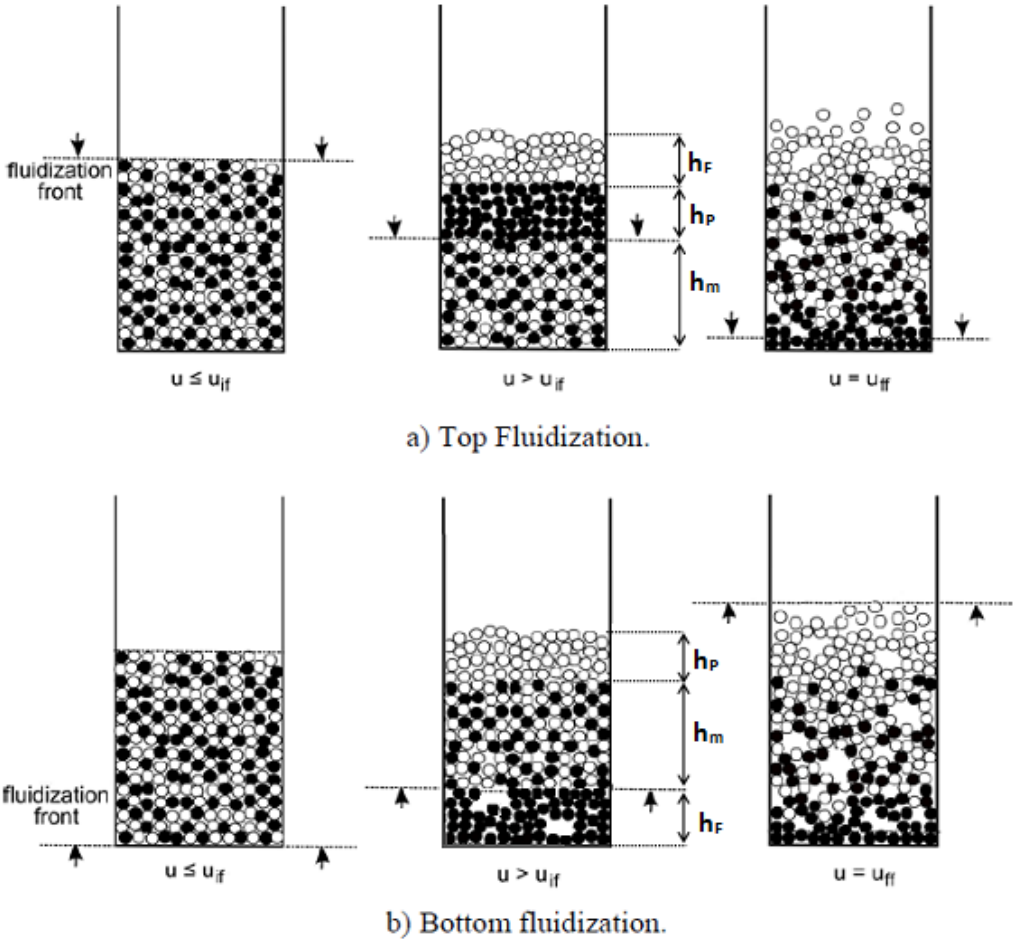


**Fig. 1: Segregating fluidization patterns**

In both cases the bed can approximately be divided into three distinct layers as u varies from $u_{if}$ to $u_{ff}$: the fluidized layer, the packed layer and the residual mixed bed, whose heights are $h_F$, $h_P$ and $h_m$, respectively. However, the mechanism of fluidization changes their order along the bed height, with the upper layer constituted by the fluidized solid or by the packed one. This three-layer structure is a good approximation of the component distribution originating from the segregation mechanisms that take place along the fluidization velocity interval.

In previous research, however, the analysis was limited to mixtures of spherical solids whereas systems of practical interest are often made of solids of irregular shape, like in operations such as coal or biomass gasification and combustion. Further investigation is therefore required to assess the model validity when non-spherical particles are involved, a goal that is pursued in the present contribution.

**THEORY**

The model tested in this work has been presented in previous papers (1,2), therefore only the basic equations are shown in this section. In its present application, however, the pressure drop is calculated by resorting to the Ergun's equation rather than to Carman-Kozeny's, in order to extend the analysis to particles with diameters larger than 1 mm. $u_{if}$ can be calculated by introducing the Sauter average diameter and the voidage of the homogeneous bed $\varepsilon_m$:

$$150\frac{\mu_g(1-\varepsilon_m)}{\varepsilon_m^3 d_{av}^2}u_{if} + 1.75\frac{\rho_g}{\varepsilon_m^3 d_{av}}u_{if}^2 = (\rho_{av}-\rho_g)g \qquad (1)$$

where

$$d_{av} = \left(\frac{1-x_F}{\phi_P d_P} + \frac{x_F}{\phi_F d_F}\right)^{-1} \qquad \text{and} \qquad \rho_{av} = \rho_P(1-x_F) + \rho_F x_F$$

The subscripts P and F refer to the packed and the fluidized solid, i.e that with the higher and the lower minimum fluidization velocity, respectively. For irregular solids, $\phi_P$ and $\phi_F$ are the particle sphericities, determined as adjustable parameters to minimize the deviation of the pressure drop data of the monocomponent packed beds from the predictions of Ergun's equation.

$u_{ff}$ is obtained by equating the pressure drop across the layers $h_P$ and $h_m$ (Fig.1) to the buoyant weight per unit section of the particles which form these two layers:

$$\left[150\frac{\mu_g(1-\varepsilon_m)^2}{\varepsilon_m^3 d_{av}^2}u_{ff} + 1.75\frac{\rho_g(1-\varepsilon_m)}{\varepsilon_m^3 d_{av}}u_{ff}^2\right]h_m + \left[150\frac{\mu_g(1-\varepsilon_P)^2}{\varepsilon_P^3 d_P^2}u_{ff} + 1.75\frac{\rho_g(1-\varepsilon_P)}{\varepsilon_P^3 d_P}u_{ff}^2\right]h_P =$$

$$= \left[(\rho_{av}-\rho_g)(1-\varepsilon_m)h_m + (\rho_p-\rho_g)(1-\varepsilon_p)h_p\right]g \qquad (2)$$

A further relationship is provided by the mass balance on component P:

$$(1-\varepsilon_P)h_P = (1-x_F)(1-\varepsilon_m)(h_0-h_m) \qquad (3)$$

The only unknown is the homogeneous bed fraction $h_m/h_0$ which can be estimated from the empirical equation:

$$\frac{h_m}{h_0} = k\frac{1-\varepsilon_m}{1-\varepsilon_P}\frac{\varepsilon_P^3}{\varepsilon_m^3}\sqrt{x_F(1-x_F)} \qquad (4)$$

where k is a best-fit parameter, which is concentration-independent and varies with the specific binary system.

## EXPERIMENTAL

Experiments were conducted in an acrylic column of 10 cm internal diameter, with a 4 mm-thick plastic porous plate as distributor. Compressed air was used as fluidizing medium, whose flow rate was measured by a bench of rotameters. A pressure tap located 1 mm above the distributor and connected to a U-tube water manometer allowed determining the total pressure drop across the bed. $u_{if}$ and $u_{ff}$ were determined from $\Delta P$ vs u diagrams at the points where the pressure drop first deviates from the fixed bed curve and $\Delta P$ attains its ultimate value, respectively.

The overall fixed-bed voidage was easily evaluated by averaging direct readings of the bed height on three graduated scales spaced at 120°C around the column wall, according to the relationship:

$$\varepsilon_0 = 1 - \frac{m_S / \rho_{av}}{A h_0} \tag{5}$$

Since only solids of Geldart's group B were employed, it was assumed that the value calculated from Eq (5) is also representative of the minimum fluidization condition. Furthermore, voidage was assumed homogeneous throughout the bed, given that all the experiments were performed on well-mixed binary mixtures. With all mixtures the aspect ratio $h_0/D$ of the fixed bed was equal to 1.7.

**Table 1: Experimental solids and mixtures**

| Solid | Density [g/cm$^3$] | Sieve size [μm] | $\phi$ [-] | $d_{av}$ [μm] | $\varepsilon_{mf}$ [-] | $u_{mf}$ [cm/s] |
|---|---|---|---|---|---|---|
| Glass beads (GB) | 2.48 | 200-300 | ~1 | 250 | 0.401 | 6.60 |
| Sand grains (SG) | 2.59 | 400-600 | 0.64 | 340 | 0.488 | 22.8 |
| | 2.59 | 200-300 | 0.60 | 160 | 0.478 | 5.60 |
| Olive pits (OP) | 1.38 | 1400-2000 | 0.80 | 1540 | 0.430 | 66.1 |

| Mixture (Packed-Fluidized) | $\rho_P / \rho_F$ [-] | $d_{av,P} / d_{av,F}$ [-] | k [-] |
|---|---|---|---|
| OP1540-SG340 | 0.53 | 4.53 | 0.092 |
| OP1540-GB250 | 0.56 | 6.16 | 0.23 |
| OP1540-SG160 | 0.53 | 9.63 | 0.057 |

Table 1 reports the properties of both the experimental solids and their mixtures. Olive pits were used as a biomass prototype and mixed with spherical glass beads or irregular sand, which is frequently employed as an inert material added to facilitate fluidization of the biomass. Compared to olive pits, sand particles showed higher deviations from the spherical shape, with one dimension often considerably longer than the others, as verified by microscopy. As a

consequence, the product $\phi$d of the sand grains was found below the lower limit of the sieving range, although their volume mean diameter fell between the sieve limits. Therefore, this effect seems due to the larger deviation associated with the strongly irregular shape of the material.

The three binary mixtures investigated exhibited top fluidization at low values of $x_F$ whereas bottom fluidization was observed at higher concentrations. This variety of behaviour represents a strong test bench for the general validity of the model proposed.

**RESULTS**

Fig. 2 presents the voidage of the homogeneous mixtures at varying solid fraction of the fluidized component. For beds of two solids differing in size, the voidage curves display a minimum at intermediate values of $x_F$ (1, 2, 7). Compared to beds of spherical particles, irregular solids form more permeable packing structures. As a consequence, the binary-solid voidage curves exhibit an increased degree of asymmetry when relevant to mixtures of particles of different shape. The monocomponent bed voidage of the solid OP1540 is slightly higher than commonly observed with spherical particles, while the sand grains form a considerably more porous assembly. As a matter of fact, higher bed voidages reflect greater deviations from the spherical shape.

Comparing the voidage contraction of the various curves of Fig. 2 is not straightforward due to the discrepancy of their extreme values. However, while for OP-SG mixtures the rate of voidage change clearly increases by reducing the diameter of sand, for the GB-OP system the percent voidage diminution, with respect to the average monocomponent voidage, is the largest, despite the size ratio relevant to this system is not the highest.

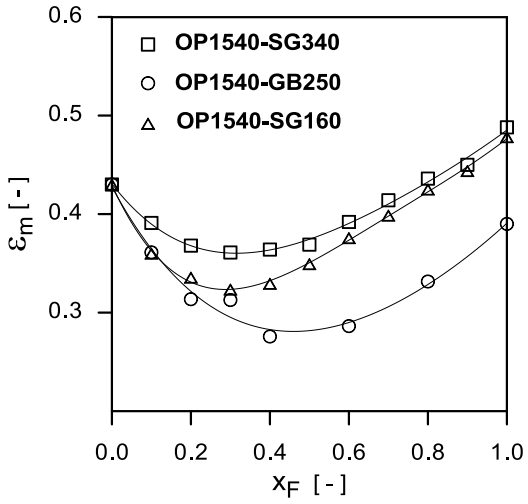


**Fig. 2: Homogeneous binary-solid bed voidage vs composition**

Thus, different from what typical of mixtures of spherical particles, the minimum of the voidage curves is not univocally related to the $d_{av}$ ratio (see Table 1), since an additional effect is played by particle shape, that gives rise to mixture voidages generally higher. As a consequence, the voidage contraction observed

for particles of irregular shape may be larger than expected with mixtures of spheres with the same component size ratio.

Fig. 3 shows $u_{if}$ and $u_{ff}$ at varying concentration for the three experimental mixtures. The shape of the fluidization velocity diagrams resembles that usually obtained for size segregating systems (1). Since all the mixtures have virtually the same density ratio (see Table 1), this result reveals that the shape irregularity does not modify the general trend of the fluidization diagram; however, it alters the transition to the fluidized state as it affects not only the product $\phi d_{av}$ but also bed voidage.

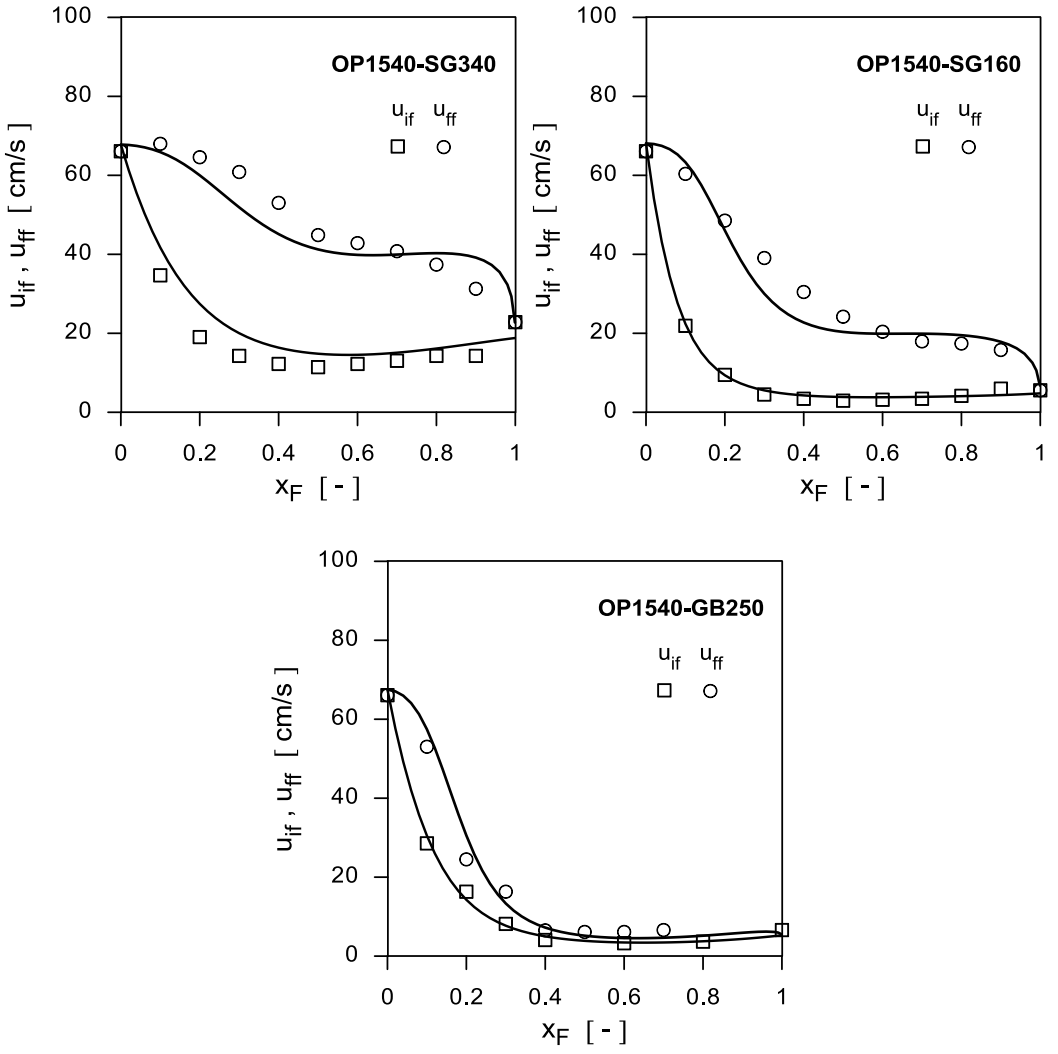


**Fig. 3: Fluidization velocity diagrams of the two-component mixtures**

The solid lines in Fig. 3 represent the model predictions from eqns (1)-(4), while the experimental values are reported as symbols. The values of k introduced in eqn (4), obtained by least squares minimization of the deviations of $u_{ff}$ from the experiments, are reported in Table 1. Inspection of eqn (4) reveals that when k results smaller the extent of segregation is larger as $h_m$ is reduced. Thus, the smallest k-value is found with the mixture having the largest size ratio, namely

with OP1540-SG160 as expected. However, the largest k is that relevant to the system OP1540-GB250, whose size ratio is not the smallest. This result seems due to the effect of particle shape on voidage. For the mixture OP1540-SG340 $\varepsilon_m$ is larger due to the strong shape irregularity of sand grains, and the value of the voidage function in eq (4) is therefore reduced. This voidage function reflects the tendency of the mixture to remain homogeneous to benefit from the gain in drag force effectiveness provided by the void condition typical of the mixed state. It can therefore be stated that low voidages and high interstitial velocities facilitate particle mixing in that they increase the drag force acting on bed components.

Although the quantitative agreement with experiments is not always excellent, the ability of the model to reproduce the velocity diagrams is remarkable, even when mixtures turn from bottom to top fluidization in response to concentration variations. More significant deviations are observed with biomass-sand mixtures which are characterized by a higher shape irregularity of their components.

## CONCLUSIONS

The velocity boundaries of the fluidization process, $u_{if}$ and $u_{ff}$, can be calculated in theoretical terms by a force balance on bed structures which reckon with the occurrence of segregation along the velocity interval that encompasses the process of bed suspension. Although the calculation of $u_{if}$ is fully predictive, that of $u_{ff}$ requires an additional one-parameter equation which quantifies the extent of segregation, to be coupled with a fundamental force balance. This parameter, endowed with a clear physical meaning, is independent of mixture concentration. It can therefore be determined by a single accurate experiment, measuring $u_{ff}$ at a known $x_F$ and then applying Eq. 4. Once that k has been calculated, $u_{ff}$ at any other concentration can be predicted, provided that the experimental trend of $\varepsilon_m$ versus $x_F$ is known.

Whatever the mechanism of fluidization, the model equations proposed prove able to interpret the fluidization behaviour of systems of solids of irregular shape with good accuracy. This corroborates the achievements of previous work, where the same relationships had been tested on systems of spherical particles differing in density and/or size. It can therefore be concluded that the model proposed provides a unified representation of the suspension process of all types of mixtures.

## NOTATION

| | |
|---|---|
| A | column cross section, $cm^2$ |
| D | bed diameter, cm |
| d | volume particle diameter, $\mu$m |
| $d_{av}$ | Sauter mean diameter, $\mu$m |
| h | height of the particle layer, cm |
| $h_0$ | height of the fixed bed, cm |
| k | best-fit parameter (Eq. 11), - |
| $m_s$ | solid mass, g |
| $u_{if}$, $u_{ff}$ | initial, final fluidization velocity, cm/s |
| x | volume fraction, - |
| $\varepsilon$ | voidage, - |
| $\varepsilon_0$ | voidage of the fixed bed, - |

| | |
|---|---|
| $\phi$ | sphericity, - |
| $\mu_g$ | gas viscosity, g/cm s |
| $\rho$ | density, g/cm$^3$ |
| $\rho_{av}$ | average density of the mixture, g/cm$^3$ |
| $\rho_g$ | gas density, g/cm |

*Subscripts*

| | |
|---|---|
| F, P | of the fluidized, packed component (or layer) |
| m | of the homogeneous mixture |

## REFERENCES


1. Formisani B, Girimonte R, Vivacqua, V. Fluidization of mixtures of two solids differing in density or size. AIChE J. 2011;57:2325–2333.
2. B. Formisani, R.Girimonte and V.Vivacqua. Fluidization of mixtures of two solids: a unified model of the transition to the fluidized state. AIChE J., 2012, in press.
3. Nienow AW, Rowe PN, Cheung LY-L. A quantitative analysis of the mixing of two segregated powders of different density in a gas fluidized bed. Powder Technol. 1978;20:89–97.
4. Rice RW, Brainovich JF. Mixing/segregation in two- and threedimensional fluidized beds: binary systems of equidensity spherical particles. AIChE J. 1986;32:7–16.
5. Wu SY, Baeyens J. Segregation by size difference in gas fluidized beds. Powder Technol. 1998;98:139–150.
6. Peeler JPK, Huang JR. Segregation of wide size range particle mixtures in fluidized beds. Chem Eng Sci. 1989;44:1113–1119.
7. Yu AB, Standish N. Porosity calculations of multi-component mixtures of spherical particles. Powder Technol. 1987;52:233–241.

**KEYWORDS**

Fluidization fundamentals; Segregation; Mixing; Binary-solid beds; Non-spherical solids.